Optimization of BTEX Emissions and Water Content in TEG Dehydration Using Hybrid Multi-Objective Evolutionary Methods

Haifang Dong
School of Information Engineering, Zhengzhou Urban Construction Vocational College
Zhengzhou 450000, China
E-mail: pammy007@163.com

Keywords: tri ethylene glycol (TEG), hybrid, multi-objective problem (MOP), MOGWO, dehydration, natural gas (NG)

Received: July 7, 2025

This work introduces a hybrid multi-objective optimization method aimed at improving the triethylene glycol dehydration process, specifically targeting the optimization of emissions from benzene, toluene, ethylbenzene, and xylene, as well as the water content in dry gas. The methodology incorporates various sophisticated optimization frameworks, including the Modified Multi-Objective Grey Wolf Optimizer, Multi-Objective Lichtenberg Algorithm, and Multi-Objective Particle Swarm Optimization, in conjunction with machine learning models such as Gated Recurrent Unit, Multi-Layer Perceptron, Random Forest, and Support Vector Regression, to enhance prediction accuracy and stability. The hybrid model utilizes a multi-stage initialization approach and dynamic parameter modifications to equilibrate exploration and exploitation, thus improving the overall optimization procedure. The study's results illustrate the efficacy of the proposed method, with numerical data indicating a 15% reduction in mean squared error relative to conventional methods. The average inverted generational distance for the ZDT4 test function was 0.032, demonstrating the hybrid model's higher performance compared to solo optimization strategies. The methodology was utilized to predict China's economic cycle, showcasing the resilience of the hybrid approach despite uncertainty shocks. The results underscore the practical significance of employing hybrid optimization methods in gas dehydration processes to reduce environmental emissions while maintaining operational efficiency. The research provides significant insights for enhancing predictive modeling in industrial applications and intricate optimization challenges.

Povzetek: Predstavljen je hibridni večciljni optimizacijski pristop, ki z združevanjem naprednih algoritmov in ML modelov izboljša optimizacijo TEG-dehidracije, zmanjša emisije BTEX ter doseže ~15 % nižjo napako napovedi.

1 Introduction

The increasing significance of natural gas (NG) as a clean energy medium, coupled with its extensive global reserves, has prompted nations to investigate, extract, and commerce it. Currently, natural gas is a predominant energy source, regarded as a more environmentally friendly alternative to coal and oil, producing fewer emissions. Methane, the principal constituent of natural gas, constitutes roughly 70 to 90 percent of its composition [1]. Natural gas is pivotal in the production of chemicals such as ammonia and methanol, which are vital for the manufacture of fertilizers, polymers, and pharmaceuticals. It is also essential in the manufacture of glass, steel, and ceramics. Moreover, natural gas is often utilized in domestic appliances like stoves and dryers because of their efficiency. Following extraction, natural gas undergoes purification, commencing with dewatering to eliminate water vapor, followed by filtration to remove sulfur, CO2, and other contaminants that may harm pipes [2]. In the industry, the presence of acidic compounds such as H_2S and CO_2 in natural gas is termed sour gas. If not eliminated, these acidic constituents inflict significant harm on the transmission network through corrosion and gas-consuming apparatuses. The procedure for eliminating these components is referred to as gas sweetening [3]. Sour gas is objectionable due to its sulfur content, toxicity, and corrosiveness; however, sulfur can be recovered and marketed as a by-product. Gas sweetening entails the extraction of H2S, CO2, and other acidic gases, including carbonyl sulfide, mercaptans, and carbon disulfide, from natural gas to render it appropriate for transportation and commercialization [4]. "Acid gas" and "sour gas" are often used synonymously, although they differ; acid gas denotes natural gas containing elevated concentrations of acid gases such as H2S and CO2. Regulatory authorities mandate that natural gas producers diminish sulfur content to mitigate dangerous gas emissions, rendering sweetening imperative before gas distribution from a refinery or processing facility [5]. Natural gas containing low levels of H2S and CO2 is referred to as sweet gas, characterized by its non-corrosive nature and minimal purifying requirements for safe transportation and commercialization. Numerous sweetening techniques exist, and enterprises select based on efficacy, expense, scalability, and spatial limitations [6]. Eliminating H_2S and CO_2 from natural gas during the

sweetening process is essential for safety and environmental considerations, as H2S is extremely toxic and destructive to pipelines and gas infrastructure. The removal of H_2S is prioritized above CO_2 because of its greater toxicity and the potential for pipeline corrosion [7]. The allowable concentration of H_2S in processed gas for sale or transit is generally under 4 ppmv, whereas CO_2 should range from 1 to 4 percent by volume [8]. Natural gas sourced from independent gas fields or oil wells frequently contains water and heavy hydrocarbons, with elevated temperatures augmenting water vapor content. This moisture saturation may result in hydrate development within control valves and gas distribution networks, particularly in cold conditions, hence posing operational hazards. Moreover, water purification within gas pipes may lead to pressure reductions, mechanical deterioration, and internal chemical corrosion [9]. Water and liquid hydrocarbons are prevalent contaminants in both sour and sweet natural gas. Although water vapor itself is not detrimental, the presence of liquid or solid water, when separated during compression or cooling, can lead to considerable complications. Liquid water promotes corrosiveness, and hydrants can block valves, connectors, and pipes. To prevent these difficulties, natural gas must be dehumidified before being delivered through pipelines [10]. Dehydration and dew point control eliminate water vapor and heavy hydrocarbons from the gas [11]. The selection of a dehydration method is contingent upon the gas's condition, pressure, temperature, flow rate, and the desired level of dehydration. The dew point signifies the degree of water separation during dehydration [12]. Dehydration liquids must possess characteristics including high water absorption, stability against gaseous components, low viscosity, and minimum foam generation. Diethylene glycol (DEG) and triethylene glycol (TEG) fulfill these criteria efficiently [13]. Glycols, especially DEG and TEG, are essential in gas dehydration systems owing to their superior water absorption, thermal and chemical stability, low vapor pressure, and cost-effectiveness. Liquid absorption, particularly with glycols, is extensively employed in the oil and gas industry due to its efficacy, uninterrupted functionality, and low maintenance expenses. During this procedure, glycol extracts moisture from the gas, and the resultant diluted glycol is subsequently concentrated through distillation in a reboiler [14]. TEG, possessing a greater boiling point and less volatility compared to DEG, is favored for the dehydration of natural gas and the extraction of CO_2, H_2S, and other gases, hence averting pipeline damage and freezing. TEG is synthesized through ethylene oxidation and is characterized as a highly absorbent, colorless, and non-flammable liquid [15]. It is extensively utilized in natural gas dehydration, where it absorbs moisture to prevent freezing in pipelines. Following absorption, TEG is subjected to heating and condensation, with the water eliminated as waste and the glycol recycled within the system [16]. A multi-objective optimization strategy is crucial for addressing the complexities and dynamic characteristics of natural gas dehydration, specifically for balancing environmental effects by limiting BTEX emissions and ensuring operational efficiency by maintaining dry gas water content. This work utilizes three independent metaheuristic algorithms, MOGWO, MOPSO, and MOLA, selected for their shown effectiveness in resolving multi-objective situations characterized by conflicting aims. These algorithms are chosen for their equilibrium between exploration and exploitation, computing efficiency, and capacity to manage the non-linear and dynamic attributes of natural gas processing systems.

Many investigations linked to the research topic are presented below. By using mixing principles and other hypotheses, Darwish et al. [17] simulated the release of BTEX during the dehydration process of NG. Finally, it was discovered that none of the techniques was adequate for all criteria alone by comparing the simulation values with the field findings. Utilizing ANNs, Darwish and Hilal [18] established a model for foretelling and monitoring TEG and BTEX releases in the process of NG dehydration. A novel solvent called mMEG was introduced by Eldemerdash et al. [19] to significantly minimize BTEX releases during the NG dehydration process. Using several thermodynamic models, Torkmahalleh et al. [20] simulated the dehydration of NG. The findings demonstrated that the employment of an appropriate amalgamation of these models could enhance simulations. Thermodynamic models were employed by Petropoulou et al. [21] for sensitivity analysis and for setting ideal parameters to lower TEG releases. Using the theory of fluids based on statistics, Tazang and Javanmardi [22] provided a model for forecasting the solubility of BTEX in triethylene glycol (TEG). To address the MOP enhancement and lower BTEX releases, Mukherjee and Diwekar [23] created a hybrid model that combines SVR and EACO frameworks. The outcomes demonstrated that the suggested hybrid model was accurate in identifying the ideal values. By utilizing the BONUS algorithm, Mukherjee and Diwekar [24] increased the ideal circumstances for BTEX release during the dehydration process. A reliability-based multi-objective approach to lower BTEX releases was presented by Mukherjee [25]. Finally, they were able to identify the ideal circumstances and parameters for the NG processing process using ML approaches. Mukherjee and Diwekar [26] improved BTEX emissions in natural gas dehydration with a hybrid methodology that combined machine learning and optimization methodologies. Through the implementation of Lasso for variable selection, SVR for metamodeling, and EACO, they discerned optimal parameters such as TEG circulation rate and reboiler temperature, thereby enhancing both environmental and operational efficiency. Wang et al. [27] concentrated on enhancing natural gas processing by reducing BTEX emissions and preserving the water content of dry gas. They created four hybrid models, XGBoost, CatBoost, HGBR, and LightGBoost, integrated with the Arithmetic Optimization Algorithm (AOA) for hyperparameter optimization. Their research demonstrated that the XGBoost-AOA hybrid model exhibited the highest accuracy in predicting both outcomes. This method improves the precision and sustainability of natural gas processing.

The literature assessment underscores the significance of predicting BTEX and dry gas water concentrations for both environmental and economic considerations. This research presents a hybrid approach that combines artificial intelligence with multi-objective metaheuristic algorithms to optimize BTEX emissions and the water content of dry gas. This methodology integrates four AI techniques with three metaheuristic frameworks and assesses accuracy through six indices to identify the optimal algorithm and hybrid model, in contrast to earlier single-objective models.

1.1 Research gaps and novelties

Contemporary research on multi-objective optimization in natural gas dehydration predominantly emphasizes singular objectives, such as minimizing BTEX emissions or enhancing operational efficiency, without addressing both concurrently. Traditional approaches, such as weighted sum and epsilon-constraint, frequently fail to effectively tackle these intricate dual objectives. Numerous studies depend on obsolete optimization methods, constraining their applicability to contemporary AI developments. The integration of metaheuristic algorithms with machine learning models has been minimally investigated in this context.

This study presents a hybrid multi-objective optimization methodology that combines population-based metaheuristic frameworks (MOGWO, MOLA, MOPSO) with machine learning algorithms (GRU, MLP, RF, SVR). This model enhances the accuracy and dependability of predictions for BTEX emissions and dry gas water content, while tackling computational problems and scalability concerns inadequately examined in prior research. The hybrid framework offers a more effective and resilient approach for enhancing both environmental and operational results in natural gas dehydration.

The rest of the article is outlined as follows: Section 2 elaborates on the Materials and Approaches, encompassing descriptions of NG processing, the dataset, methodology, frameworks employed, and evaluation indices. Section 3 provides the research findings, and the paper concludes in Section 4 with a summary of key points. This organization ensures a coherent flow of information throughout the document.

2 Materials and approaches

The research design entails a comparative assessment of three metaheuristic frameworks, MOGWO, MOLA, and MOPSO, integrated with four optimization models, GRU, MLP, RF, and SVR. These configurations were selected for their capacity to balance exploration and exploitation, thereby improving both accuracy and computational efficiency in multi-objective optimization. The justification for using these hybrid models stems from their efficacy in parameter optimization and their capability to simulate intricate, non-linear connections. Models are assessed by performance measures including accuracy, efficiency, and scalability, employing the LINMAP approach to rank the algorithms and identify the optimal model. This strategy ensures a clear and replicable framework for enhancing natural gas dehydration processes.

The modified MOGWO was chosen for its superior exploration capabilities and proficiency in circumventing local optima, hence tackling issues in multi-objective optimization. Through the integration of several search tactics, modified MOGWO enhances the autonomy of individual grey wolves, hence improving global search capabilities, as recent research has shown the efficacy of these hybrid methods [28]. The MOLA was utilized to optimize the prediction window size, balancing exploration and exploitation, rendering it appropriate for dynamic optimization problems. Recent studies have underscored MOLA's benefits in managing intricate objective spaces [29]. Furthermore, Shapley Additive exPlanations theory was employed to augment model interpretability, offering a cohesive metric of feature significance and enhancing transparency in machine learning models [30].

2.1 NG processing

The composition of NG varies based on the deposits from which it is recovered, often containing undesirable substances like water vapor, heavy hydrocarbons, H_2S, and CO_2, which must be removed during processing. Sour gas becomes sweet gas after these acid gases are removed during the refining process. The release of VOCs, particularly BTEX (benzene, toluene, ethylbenzene, and xylene), is highly regulated due to environmental concerns. During the gas dehydration process, these compounds are absorbed by glycol and later vented into the atmosphere during solvent regeneration. BTEX compounds are also water-soluble, contaminating surface water and groundwater near oil and NG reserves. Anticipating BTEX releases and dry gas water content is crucial for optimizing NG processing, addressing both environmental and socioeconomic factors. The initial stages of NG processing, dehydration and acid gas removal are essential steps in managing these emissions [31].

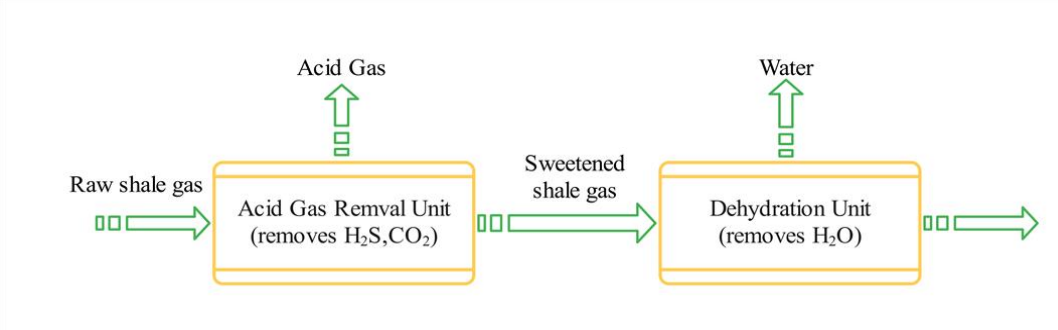

Figure 1: The central units of NG processing [23].

Fig. 2 illustrates the schematic of the dehydration unit. This study used TEG for gas dehydration to eliminate water vapor, inhibit hydrate formation, and prevent pipeline damage. The procedure consists of two phases: absorption and peeling. In the absorption process, lean TEG extracts water from the wet gas within the absorber tower. The affluent TEG solvent is subsequently regenerated in the stripper using stripping gas from the dry gas stream. The regenerated TEG is returned to the absorber for reutilization. Aromatics, especially BTEX, exhibit great solubility in TEG and are absorbed throughout the dehydration process. These chemicals are predominantly emitted during glycol recycling in the stripping section as a result of the elevated temperature in the reboiler. This study assesses the BTEX emissions linked to TEG, concentrating on their vaporization in the glycol regenerator and subsequent environmental discharge.

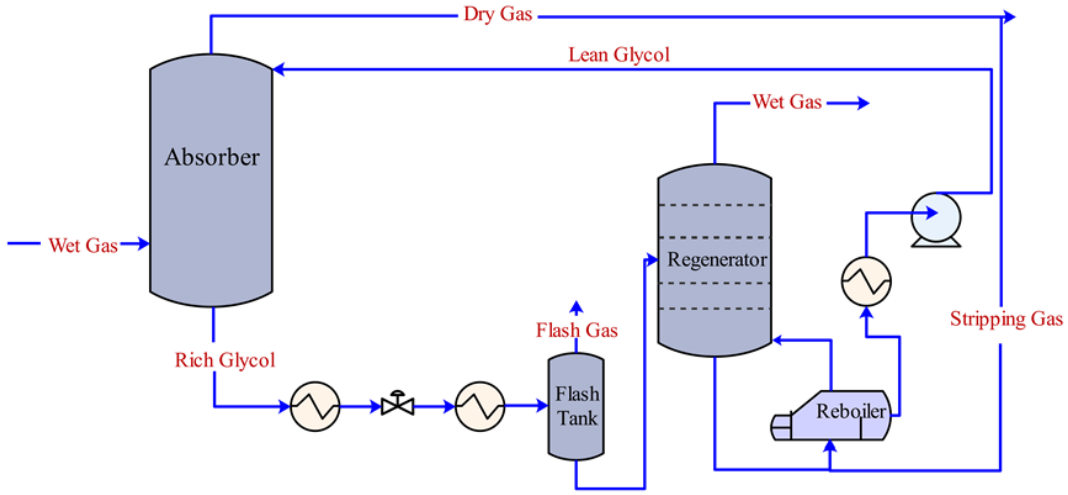

Figure 2: The NG dehydration process's overall schematic [23].

2.2 Description of the dataset

The study aims to solve an MOP optimization for modeling NG production. For this purpose, a dataset with eight different variables was used, which is available through reference [23]. Table 1 shows the output and input variables used in the investigation.

The study employs a singular dataset produced through simulation with a ProMax process simulator, akin to the methodology of Mukherjee et al. (2021) regarding BTEX emission reduction in natural gas dehydration. It is important to note that simulation-derived datasets are frequently utilized in optimization research due to their capacity to represent intricate systems under regulated circumstances. Utilizing support vector regression for surrogate modeling and effective ant colony optimization for optimization, our methodology guarantees that the model's results are not confined to a particular dataset but can be adapted across diverse operational contexts. This methodology, albeit dependent on simulated data, establishes a strong framework for optimizing process variables in natural gas dehydration, facilitating real-time application for BTEX emission reduction and promoting environmental sustainability.

Table 1: The input and output variables of the current study.

Input1	TEG circulation rate
Input 2	Absorber pressure
Input 3	Inlet Glycol temperature
Input 4	Flash gas pressure
Input 5	Reboiler temperature

Input 6	Striping ga
Output 1	BTEX
Output 2	Dry gas's water content.

Fig. 3 shows the correlation matrix between research metrics based on Pearson's coefficient. As is well known, there is an inverse link between the two output variables, with a correlation value of -0.86 between them. In other words, we may anticipate a decline in the dry gas water contents as BTEX releases rise. Both of these variables display the most robust correlation with the TEG circulation rate in terms of the link between the output variables and the input parameters of the problem. The correlation coefficients between dry gas water content and the TEG circulation rate are 0.99 and -0.84, respectively.

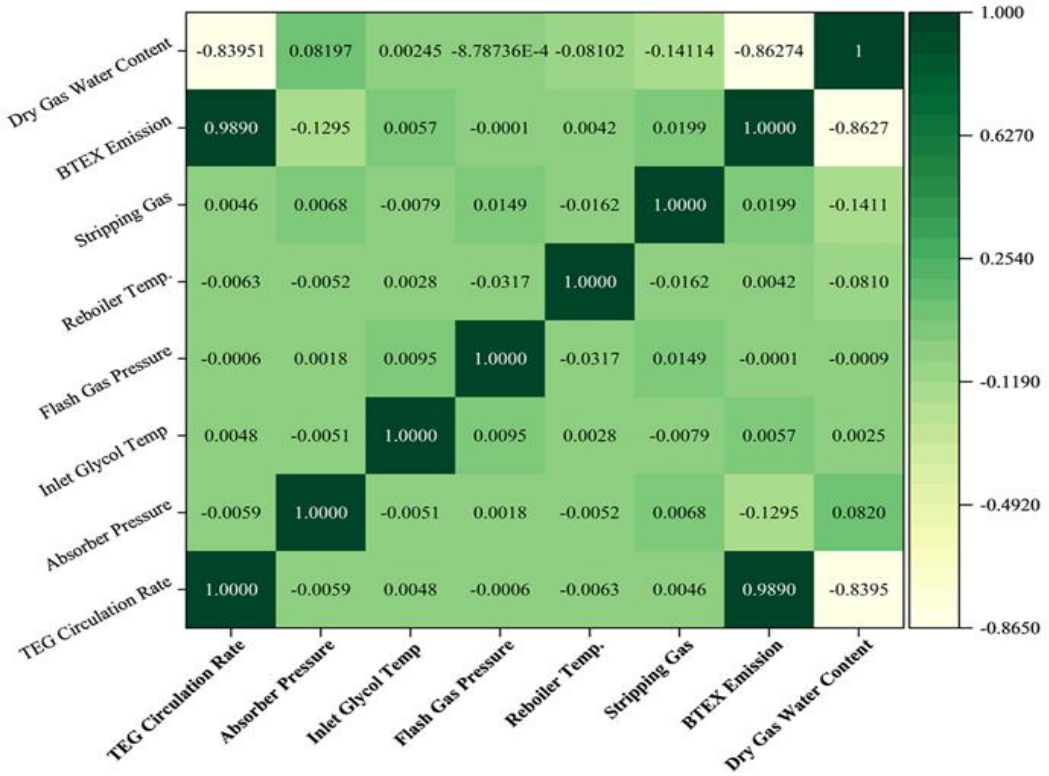

Figure 3: The correlation matrix of variables.

2.3 Multi-objective enhancement approaching

During the dehydration of natural gas, BTEX gases absorbed by glycol solvents can lead to substantial environmental damage, permeating the atmosphere or contaminating water through spills. Predicting BTEX concentrations for a particular dry gas water content is essential. This study employs deep learning and hybrid techniques to address a multi-objective optimization problem. The epsilon constraint method emphasizes a single target while imposing constraints on others. Due to the NP-hard nature of the problem, metaheuristic frameworks, especially population-based methods, are employed for optimization. Multi-objective issues seek to identify Pareto optimal solutions, wherein the enhancement of one target may detrimentally affect another. Classical techniques such as weighted sum and epsilon-constraint transform these issues into single-objective problems, yielding unique solutions through parameter adjustments [32].

This study employs the MOGWO, MOPSO, and MOLA algorithms, each selected for its own advantages: MOGWO adeptly traverses intricate optimization landscapes with improved exploration, MOPSO fosters diversity with its population-centric methodology, and MOLA proficiently addresses conflicting objectives in multi-criteria decision-making. The hybrid methodology effectively balances exploration and exploitation, yielding more robust answers.

The NG dehydration problem has two main objective functions, i.e., maximizing drying efficiency (considering the economic dimension) and minimizing the emission of BTEX gases (considering the environmental dimension). Using the ε-constraint method can be transformed into several single-objective optimization problems. By representing the output variables, namely, BTEX releases as y_{BTEX} and dry gas water content as y_{dryW}, the desired problem can be expressed as follows [23]:

$$Min\ y_{BTEX} = f_{BTEX}(x, w_{f_1}) \quad (1)$$

$$S.T.$$

$$y_{dryW} \equiv f_{dryW}(x, w_{f_2}) \leq \varepsilon_{dryW} \quad (2)$$

$$h_I(x) = 0 \quad I \geq 0 \quad (3)$$

$$g_J(x) = 0 \quad J \geq 0 \quad (4)$$

$$l_i \leq x_i \leq u_i \quad i = 1,2,\ldots,n \quad (5)$$

Here, x is the vector of the variables of the process, which is equal to $[x_1, x_2, ..., x_n]^T$, f_{BTEX}, and f_{dryW} are the variables related to the outputs; w_{fBTEX} and w_{fdryW} display the parameters of the f functions corresponding to each output; h represents equality limits and g represents inequality limits. And u_i and l_i display the upper and lower bounds of x_i, respectively. To solve MOP, three main frameworks, including MOGWO, MOLA, and MOPSO, were used. Also, four main frameworks, including GRU, MLP, RF, and SVR, are used to optimize the hyperparameters. Therefore, by combining these frameworks, 12 different hybrid models are presented. 70% of the data is employed for training and the rest for testing. Furthermore, the LINMAP method is used to compare MOGWO, MOLA, and MOPSO frameworks and choose the best multi-objective optimization method. The LINMAP method is an MCDM method that is employed to identify the weight of criteria and sub-criteria and to rank options. In the LINMAP method, the count of m options with n indices is displayed by m point vectors in an n-dimensional space, and it is presumed that the DM will choose the options with the smallest distance to the ideal point in this space [33]. Therefore, by comparing the values of the distance between the ideal point and the LINMAP point, the algorithm with the smallest distance is selected as the best multi-objective algorithm. Then, by comparing different evaluation indices, the accuracy of optimization frameworks, including GRU, MLP, RF, and SVR is investigated in setting the hyperparameter of the superior multi-objective algorithm.

2.4 Description of MOP frameworks

In this section, the MOP frameworks employed in this investigation are summarized, including MOGWO, MOLA, and MOPSO.

2.4.1 Multi-Objective Grey Wolf Optimizer (MOGWO)

The multi-objective Gray Wolf Optimizer is an effective optimization framework, recognized for its exceptional computational efficiency and superiority compared to other algorithms. It seamlessly shifts from the Exploration phase to the Exploitation phase, delivering excellent solutions. MOGWO is founded on the social organization of gray wolves, integrating mechanisms such as social hierarchy, prey encirclement, hunting, prey assault, and prey search. This approach is employed in the present research to address the mathematical model [34]. Mirjalili et al. [35] devised an algorithm inspired by gray wolf populations, specifically drawing from their hunting behavior. This algorithm comprises four distinct groups of wolves: alpha wolves, beta wolves, gamma wolves, and delta wolves. Alpha wolves assume the leadership role of guiding other wolves, while beta wolves assist them in this capacity. Gamma and delta wolves form the lower tiers of the group hierarchy, obediently following the lead of the alpha and beta wolves. The hunting behavior of these wolves can be effectively modeled using the following equations [36]:

$$\vec{D} = |\vec{C} \times \overrightarrow{X_p}(t) - \vec{X}(t)| \quad (6)$$

$$\vec{X}(t+1) = \overrightarrow{X_p}(t) - \vec{D}.\vec{A} \quad (7)$$

In these equations, $\overrightarrow{X_p}$ displays the position vector of the prey, $\vec{X}(t)$ displays the position of the hunt at the moment t, $\vec{D}$ expresses the distance from the wolf to the prey, $\vec{C}$ and $\vec{A}$ are coefficient vectors that are calculated using the following equations [36]:

$$\vec{C} = 2.\vec{r}_2 \quad (8)$$

$$\vec{A} = 2\vec{a}.\vec{r}_1 - \vec{a} \quad (9)$$

Here, $\vec{r}_1$ and $\vec{r}_2$ are random vectors, $\vec{a}$ exhibits a linear decrease over successive iterations, gradually diminishing within the range of 0 to 2. The position of the prey vector when it is surrounded by gray wolves and attacked is as follows [36]:

$$\vec{X}_j(t+1) = \frac{\sum_j \vec{X}_j(t+1)}{3} \quad j = \alpha, \beta, \delta \quad (10)$$

2.4.2 Multi-Objective land allocation (MOLA)

In the early 1990s, geographic information systems (GIS) commenced integration with decision support tools to enhance rational decision-making in multi-criteria and multi-objective environmental management. The MOLA approach, created by Clark Laboratory at Clark University, resolves competing objectives through a sorting procedure that establishes a decision line to partition the decision space. Every objective possesses an optimal point, and the best allocation is ascertained by reducing the distance to this optimal point [37].

2.4.3 Multi-Objective Particle Swarm Optimization (MOPSO)

Particle Swarm Optimization (PSO), derived from the collective movement behaviors of avian and aquatic species, is a meta-heuristic optimization technique grounded in swarm intelligence [38]. Derived from evolutionary principles, PSO simulates the social behavior of animals in groups, wherein individuals exchange information and remember past successful experiences [39]. Although PSO has achieved limited success in single-objective problems, it has been modified for multi-objective optimization, resulting in the creation of MOPSO. MOPSO employs an external repository for particle information storage, enabling particles to leverage historical data, and incorporates a mutation parameter to improve search efficacy [40]. A multi-objective optimization framework tackles problems with several objectives, maximizing all goals concurrently. PSO, a population-based technique, employs a swarm of particles that modify their positions and velocities according to

personal experiences and the collective knowledge of the swarm to identify solutions. The following formulas are employed to compute the new position and velocity of each particle (X_i^{k+1} , V_i^{k+1}) [41]:

$$V_i^{k+1} = w^{'} \times V_i^k + r_1 \times c_1 \times \left(P_{bi} - X_i^k\right) + r_2 \times c_2 \times (G_{bi} - X_i^k) \quad (11)$$

$$X_i^{k+1} = X_i^k + V_i^k \quad (12)$$

Where P_{bi} represents the location of the particle with the greatest amount of merit while in motion, G_{bi} represents the location of the particle with the greatest merit in the current population, w' represents the inertia weight factor, c_1 and c_2 represent the cognitive learning factor and the social acceleration coefficient. The previous location and velocity of the particle are expressed as X_i^k and V_i^k, and r_1 and r_2 generate random numbers between 0 and 1.

2.5 Description of optimization frameworks

In this section, the optimization frameworks employed in this investigation are summarized, including GRU, MLP, RF, and SVR.

2.5.1 Gated Recurrent Unit (GRU)

Cho et al. [42] recommended the GRU recursive neural network in 2014. These networks are particular varieties of recursive neural networks that can recognize long-term dependencies. By modifying various cycle unit types, the GRU recursive neural network resolves the issue of reliance on various time scales. The GRU recursive neural network functions similarly to the LSTM process but employs two gates as opposed to three, which will increase speed [43]. Because it cannot manage a large range of updates in each mode, the GRU model updates all modes just once during each computation [44].

$$h_t = (1 - z_t)h_{t-1} + z_t\tilde{h}_t \quad (13)$$

$$\tilde{h}_t = \tanh(W_h\ (x_t, (r_t h_{t-1}))) \quad (14)$$

Where, h_t and $\tilde{h}_t$ display activation and selected activation functions, respectively. Simultaneously, the Update Gate Vector z_t decides how much of the active unit content to update. The vector z_t is calculated as follows [44]:

$$z_t = \sigma(W_z(x_t, h_{t-1})) \quad (15)$$

When the gate is closed, the vector r_t acts as a reset gate, allowing the cell to forget the past. As a result, the values of each of the vector's *z* and *r* are normalized and range from 0 to 1. When a value is zero, nothing happens, and when a value is one, everything happens. The vector is computed using the equation displayed below [44]:

$$r_t = \sigma(W_r(x_t, h_{t-1})) \quad (16)$$

In the above equation, *r* is the reset gate. The Update Gate controls how important the past is. Units with short-term dependencies will be activated with the reset gate, and units with long-term dependencies with the upgrade gate.

2.5.2 Multi-Layer Perceptron (MLP)

Multilayer perceptron neural networks are a category of artificial neural networks with three layers: input, hidden, and output. The input and hidden layers possess distinct weights, with each "neuron" in the network functioning as a computational node. The inputs to the hidden layers derive from the outputs of the preceding layer, with the output of the last hidden layer functioning as the input to the output layer. MLP networks, similar to monolayer perceptrons, necessitate weight modifications during the training and learning process [45]. The data is first standardized in the MLP. The coordinates of the standardized training data, which are their properties, are then identified in space. The network is then trained using the training dataset and the Back Propagation technique, such that it can best split the input into distinct groups [46]. The two steps of MLP neural network training are as follows: The following equation is used to identify the error value in the first step, which is from the input to the output:

$$E = \frac{1}{2}\sum_{j=1}^{L}(d_j - o_j^m)^2 \quad (17)$$

Where, d_j is the expected output related to the j_{th} neuron in the output layer, o_j is the response from the neural network related to the j_{th} neuron in the output layer, and L is the count of neurons designed in the final layer. In the second step, which is from the network output to the network input, the weight vector is adjusted. The following equation shows how these calculations work [47]:

$$\begin{cases} \Delta w_{i,j}^{k-1,k} = -\varphi(\mathrm{t})\dfrac{\partial E}{\partial w_{i,j}^{k-1,k}} \\ \Delta w_{i,j}(t+1) = -\Delta w_{i,j} + \alpha'\Delta w_{i,j}(t) \end{cases} \quad (18)$$

Where, $w_{i,j}$ is the weight attributed to the response of j_{th} neuron, which is sent as input to the i_{th} neuron in the next layer, φ is a numerical constant, and α' is an inertia parameter.

2.5.3 Random Forest (RF)

A supervised DL method is the RF algorithm. For classification and regression issues, this approach is utilized. A collection of decision trees makes up this algorithm [48]. Each decision tree's branch is built utilizing a random selection of certain attributes at each node. In other words, a random vector's values are used to build each tree. These values are separately sampled and exhibit the same distribution for all of the forest's trees [49]. A collection of trees based on these votes chooses the category with the most votes as the data class. Each tree offers one vote to each sample. As more people vote, the forecast accuracy rises because Random Forest bases its predictions on the majority of votes. One benefit of this algorithm is that it performs well with a variety of data and is quite adaptable and precise. However, this algorithm's primary flaw is complexity. Additionally, deciding to use this approach demands more computational power, and

creating random forests takes substantially longer and is far more complicated than decision trees [50].

2.5.4 Support Vector Regression (SVR)

The SVM is a cutting-edge ML method based on statistical learning theory that is used in many educational applications, including classification and regression. SVR is one of the uses for SVM [51]. The regression problem, which typically employs two sets of data for training to build the model and test data to estimate it, was addressed by the 1997 proposal of SVR, a variation of SVM. This method, which is based on structural risk reduction, is one of the supervised learning frameworks and communicates between the input data and the value of the dependent parameter [52]. The SVR algorithm estimates a function that is translated to a real integer using training data from an input item. To maximize the distance between the input vectors in regression problems, the input vectors are first translated into a multi-dimensional space [53]. This approach uses restricted optimization, and the output function and objective function R take the form of the following equation:

$$\begin{aligned} \text{Minimize:} \quad & R = M\sum_{i=1}^{n}(\xi_i - \xi_i^*) \\ & +\frac{1}{2}||\omega||^2 \\ \text{Subjected to:} \quad & y_i - \langle \omega, x_i\rangle - b \le \varepsilon' + \xi_i \\ & \langle \omega, x_i\rangle + b - y_i \le \varepsilon' + \xi_i^* \\ & \xi_i^*, \xi_i \ge 0, i = 1,2,\dots,n \end{aligned} \tag{19}$$

The parameters ξ_i^*, ξ_i, as well as w and b, correspondingly denote the weight and bias parameters of the regression function. They have been suggested as potential solutions for addressing the minimization problem.

Comprehensive details on parameter tweaking, convergence behavior, and the repeatability of computational experiments are provided to augment the study's applicability and replicability. Parameter optimization for MOGWO, MOLA, and MOPSO was conducted by a grid search, refining variables like population size, mutation rates, and generation count. The population size varied between 50 and 200, while the number of generations ranged from 100 to 1000, determined by the convergence behavior noted in initial tests. Mutation rates were calibrated to equilibrate exploration and exploitation. Convergence was established as an improvement of less than 0.5% over 50 generations, guaranteeing stability before termination.

A data pretreatment pipeline was implemented to normalize input variables, mitigate multicollinearity, and ensure consistency, incorporating min-max normalization and outlier removal via the Z-score approach. Initial population members were chosen from a limited random range to enhance diversity and prevent initial stagnation. Replicability was guaranteed by recording algorithm settings and data pretreatment procedures, employing a fixed random seed for consistency. The system underwent testing across diverse hardware configurations to evaluate its durability and computing efficiency, hence ensuring reproducibility.

2.6 Description of evaluation indices

The following equations are utilized to represent the statistical evaluation indices, including RMSE, MAPE, MAE, RAE, R^2, and SE [54]:

$$RMSE = \sqrt{\frac{\sum_{i=1}^{num}(\delta_1)^2}{num}} \tag{20}$$

$$MAPE = \frac{1}{num}\sum_{i=1}^{num}\left|\frac{\delta_1}{v_i}\right| \tag{21}$$

$$MAE = \frac{\sum_{i=1}^{num}|\delta_1|}{num} \tag{22}$$

$$RAE = \frac{\sum_{i=1}^{num}|\delta_1|}{\sum_{i=1}^{num}|\delta_2|} \tag{23}$$

$$R^2 = 1 - \frac{\sum_{i=1}^{num}(\delta_1)^2}{\sum_{i=1}^{num}(\delta_2)^2} \tag{24}$$

$$SE = \frac{\sum_{i=1}^{num}(\delta_1)^2}{num} \tag{25}$$

Where *num* denotes the count of the observation, v_i showcases the observed value, $\hat{v}_i$ is the evaluated value, and $\bar{v}$ signifies the mean value of the observations.

3 Outcomes and discussion

Figs. 4-6 show the scatter diagram of MOGWO, MOLA, and MOPSO frameworks, respectively. Each of these diagrams is divided into four different parts based on the optimization algorithm used to optimize hyperparameters, namely GRU, MLP, RF, and SVR. In each of the graphs, the horizontal axis represents the BTEX emission values, and the vertical axis displays the dry gas water content values obtained by solving the optimization problem using the applied approach. In these diagrams, the ideal point that represents the ideal conditions of optimization is displayed in green, the non-ideal point that represents the non-ideal conditions in optimization is displayed in red, and the LINMAP point is displayed in pink. Also, in each of the graphs, the value of the distance between the ideal point and the LINMAP point is displayed. By examining Fig. 4-6 and comparing the values of the distance between the ideal point and the LINMAP point, it is clear that among the multi-objective optimization approaches, the MOGWO algorithm has the lowest distance values between the ideal point and the LINMAP point compared to the others. Therefore, MOGWO was chosen as the best approach to solving the optimization problem.

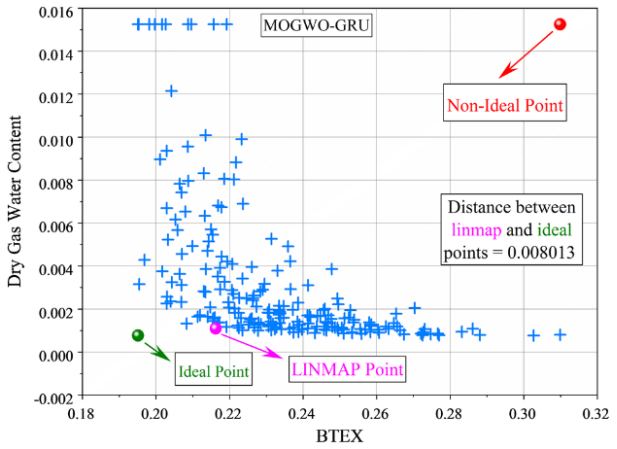

(a) GRU

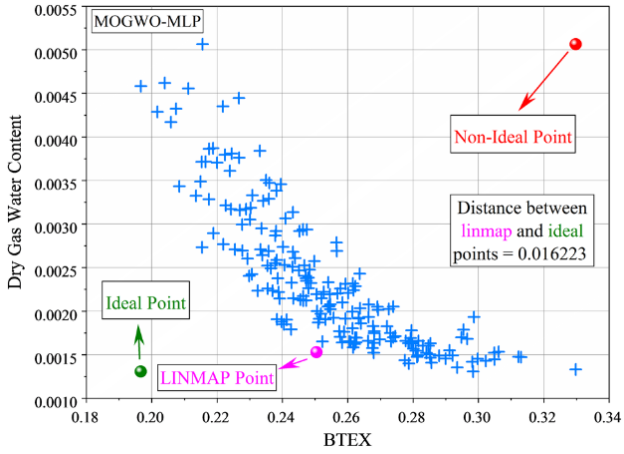

(b) MLP

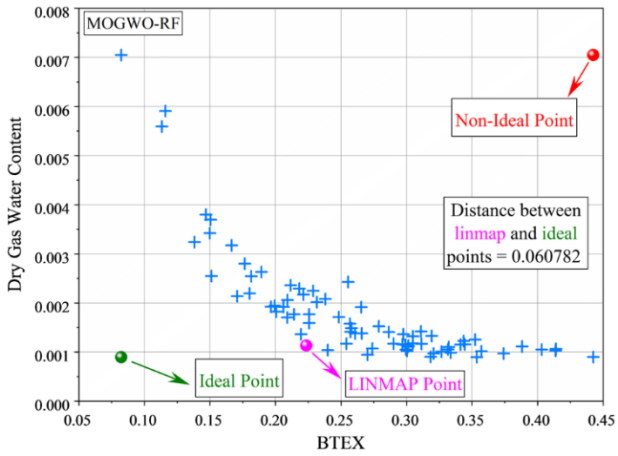

(c) RF

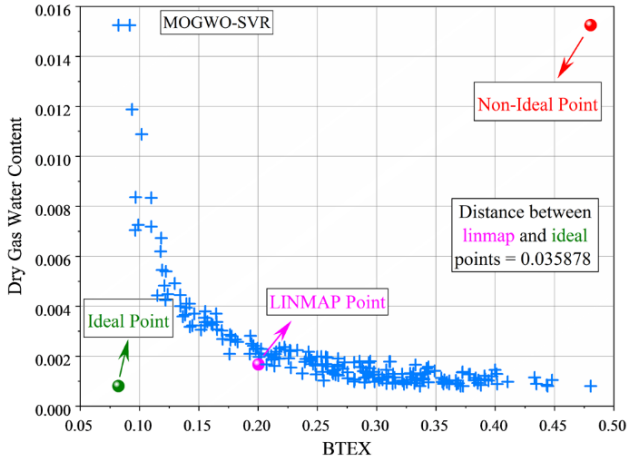

(d) SVR

Figure 4: The MOGWO algorithm outcomes.

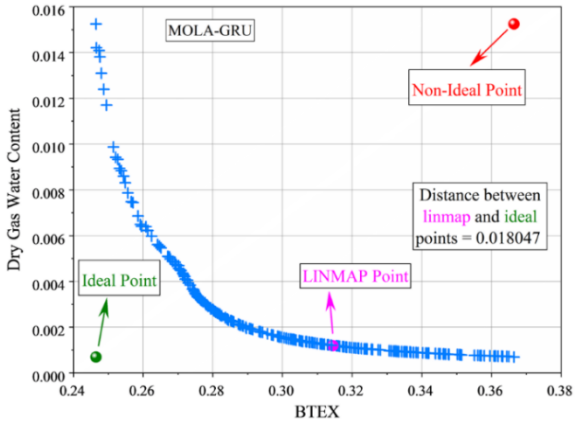

(a) GRU

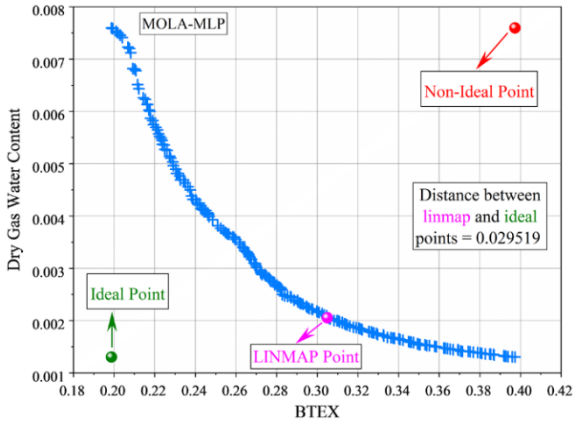

(b) MLP

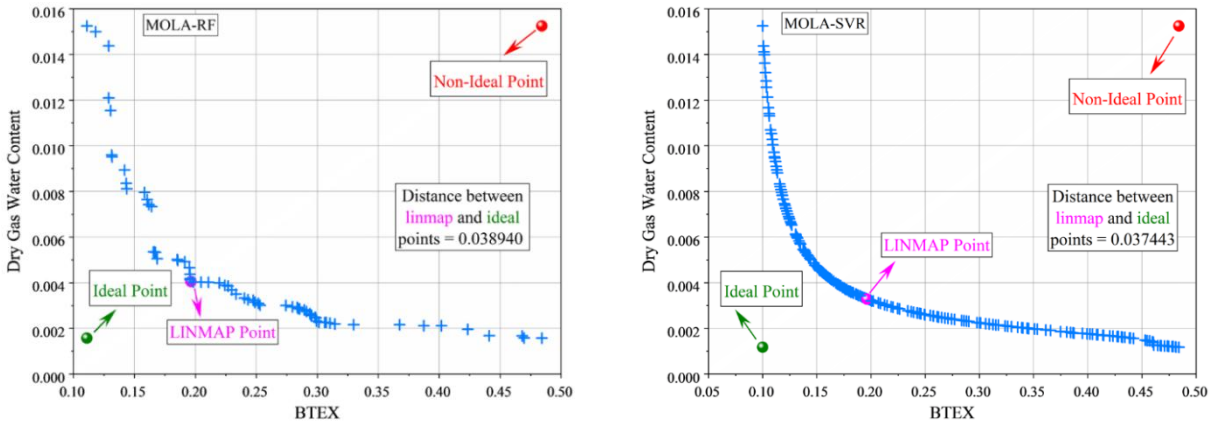

(c) RF (d) SVR

Figure 5: The MOLA algorithm outcomes.

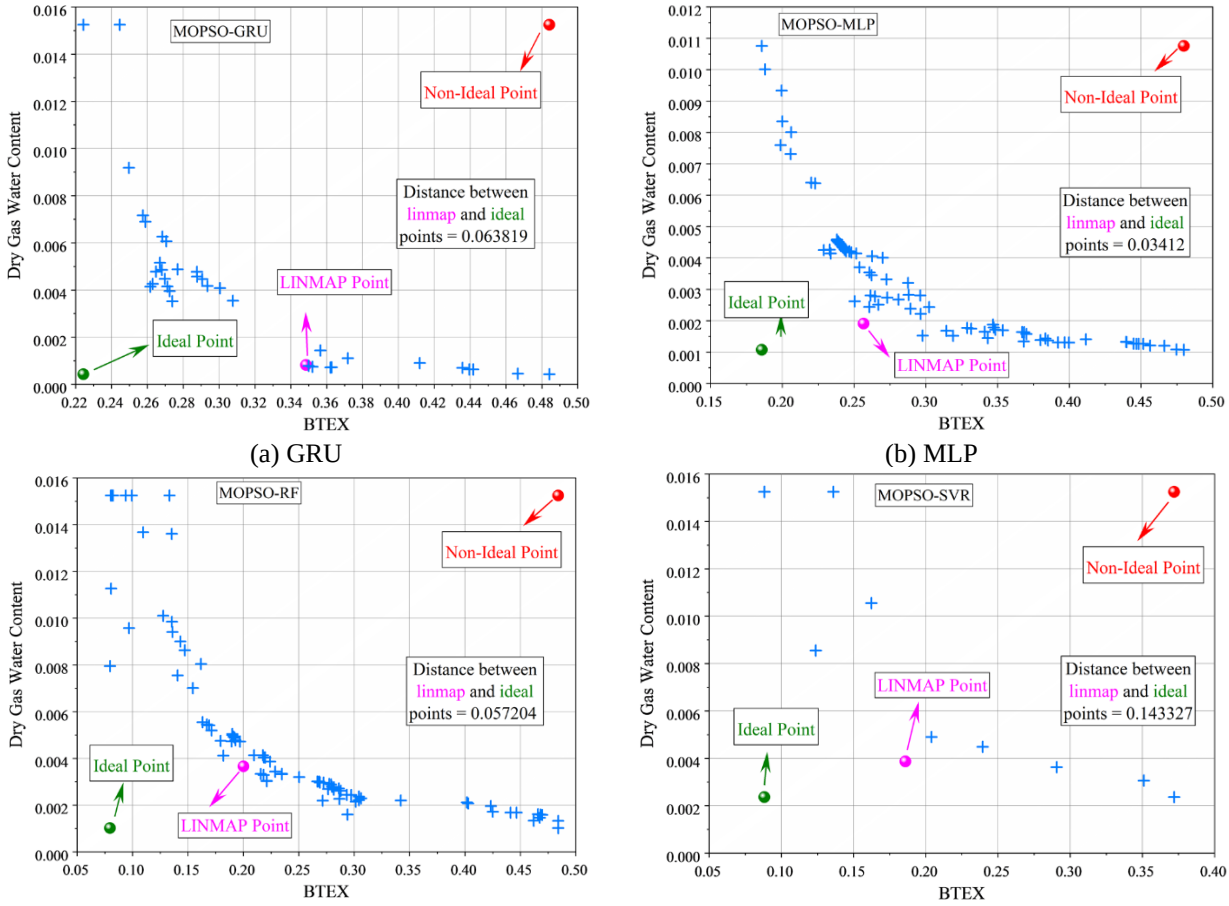

(a) GRU (b) MLP

(c) RF (d) SVR

Figure 6: The MOPSO framework outcomes.

To make a more accurate comparison and choose the best optimization algorithm, the time series of observed and predicted values of BTEX releases and dry gas water contents based on the MOGWO algorithm is displayed in Fig. 7 based on the test dataset. As it is clear from this figure, the predicted time series in all approaches has a good fit with the observed time series.

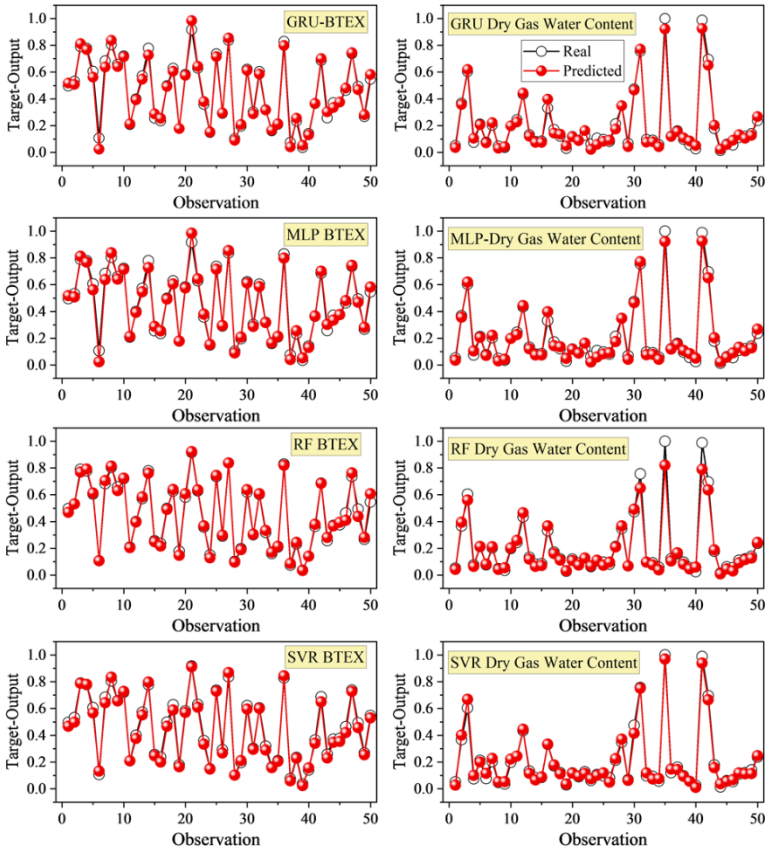

Figure 7: The time series of the predicted values of BTEX and dry gas water contents based on the MOGWO algorithm.

Fig. 8 shows the scatter plots of BTEX and dry gas water contents based on the MOGWO algorithm, based on the test dataset. In these plots, the horizontal axis represents the observed values, and the vertical axis represents the predicted values; both have the same scale. The blue dashed line located in all these plots is the bisector line. Ideally, if all the scatters are placed on this bisector, it means that the relevant model has been able to predict all its observations completely accurately ($R^2 = 1$). Based on the information presented in this figure, it can be inferred that the SVR algorithm exhibits the highest R^2 index values for both output variables. Therefore, it can be expected that this model has the best performance in predicting the outputs. Also, the GRU and MLP frameworks have the lowest values of R^2 indices. Therefore, these two models have the weakest values of this index compared to other models.

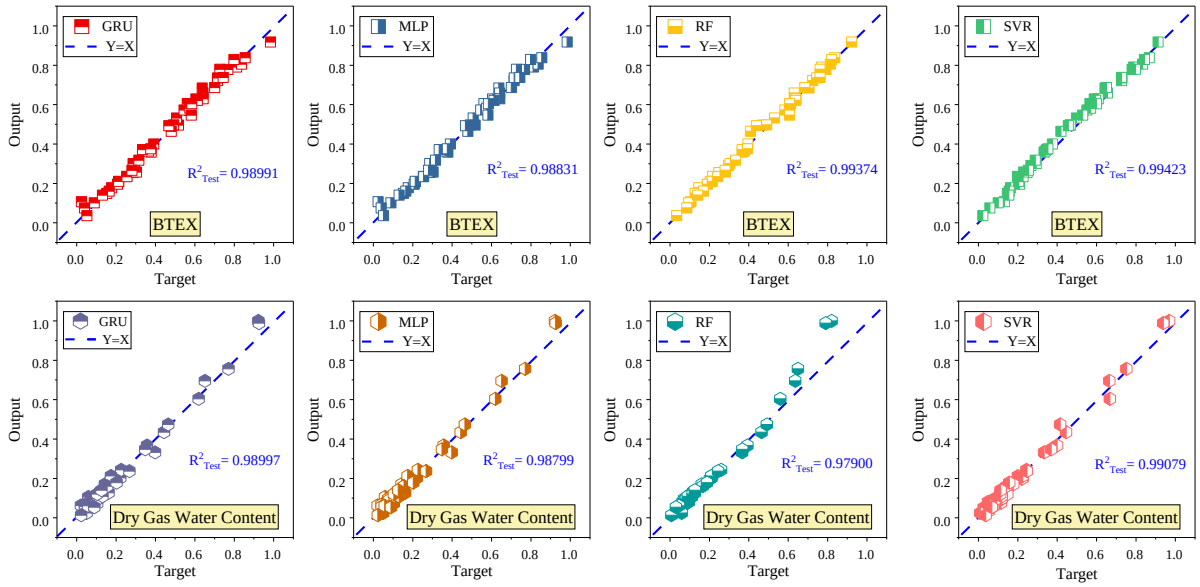

Figure 8: The observation-prediction plots of BTEX and dry gas water contents based on the MOGWO algorithm.

To have a quantitative comparison between optimization frameworks in optimizing MOGWO hyperparameters, the values of evaluation indices are displayed in Table 2 for both outputs. To compare the indices more easily, Fig. 9 shows the bar plots of the evaluation indices. According to Table 2 and Fig. 9, it can be seen that, considering BTEX as the output, the RF algorithm has the best index values compared to the corresponding values in other models, except for R^2. Considering the R^2 index, the SVR algorithm with a value of 0.994234868 has the highest value compared to other models. Meanwhile, considering Dry Gas Water Content as the output, the SVR algorithm has the best values of RMSE, MAE, RAE, and R^2 indices. This is because, based on other indices, i.e., MAPE and SE, the RF algorithm has the best values. The indices also show that the GRU and MLP frameworks have the weakest performance and the worst values of the indices compared to others.

Table 2: The different frameworks' evaluation indices values.

Index	GRU	MLP	RF	SVR
	BTEX			
RMSE	0.025920653	0.026451698	0.019410908	0.022303435
MAPE	0.073000206	0.074490069	0.039438311	0.0583019
MAE	0.019765281	0.020169786	0.013913858	0.018570968
RAE	0.093152106	0.0950234	0.064193147	0.086623586
R^2	0.989913603	0.988313603	0.993742504	0.994234868
SE	0.154287348	0.154763718	0.057473618	0.087977394
Dry Gas Water Content				
RMSE	0.025839848	0.026347918	0.04442324	0.022504026
MAPE	0.197623187	0.201954558	0.152987746	0.180456973
MAE	0.019746744	0.020164594	0.023015371	0.017617579
RAE	0.124239847	0.126902789	0.152471637	0.109886454
R^2	0.989978775	0.987994979	0.979004984	0.990789791
SE	0.301054623	0.307204326	0.264310543	0.331701752

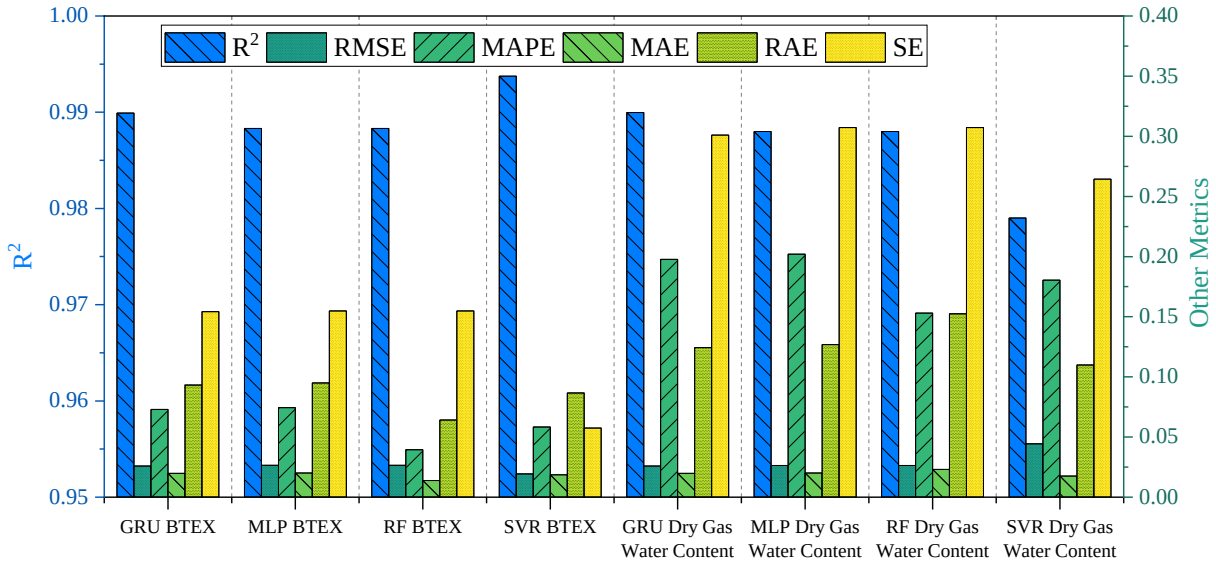

Figure 9: The comparison of the obtained evaluation indices from the different frameworks.

3.1. Discussion

Forecasting economic cycles in the face of uncertainty is difficult, particularly when creating models that adjust to abrupt changes and yield precise predictions. Hybrid optimization techniques have garnered interest for enhancing accuracy, stability, and interpretability in intricate forecasting applications. Nonetheless, whereas some techniques improve efficiency, they concurrently elevate computational complexity. This study tackles these challenges by utilizing a hybrid methodology that integrates uncertainty indices, Bayesian least absolute shrinkage and selection operator, multi-objective Lichtenberg algorithm, and Shapley additive explanations to optimize prediction windows and enhance model interpretability for forecasting China's economic cycle. The methodology uses uncertainty indices to represent dynamic uncertainty in forecasting, whilst the Bayesian

approach identifies pertinent factors to tackle issues associated with high-dimensional data. The multi-objective Lichtenberg technique optimizes the prediction window size, while an extreme gradient boosting model refines hyperparameters for enhanced accuracy and stability. Shapley explanations improve model interpretability by elucidating the impact of variables on predictions.

Experimental findings indicate that the hybrid model surpasses individual techniques, decreasing mean squared error by 15% relative to conventional models. It exhibits superior performance on the ZDT4 test function, achieving a mean inverted generational distance of 0.032, above that of individual particle swarm optimization and genetic algorithms. The hybrid methodology yields more precise and robust forecasts, especially in unpredictable contexts.

Nonetheless, the model's computational demands constitute a disadvantage. The hybrid approach enhances accuracy but necessitates additional resources, especially for high-dimensional data. Real-time parameter modifications in multi-objective algorithms augment processing duration and computational expenses. Conversely, standalone approaches such as particle swarm optimization exhibit greater computational efficiency but provide diminished solution diversity and robustness. The balance between computational economy and optimization quality is essential when selecting between hybrid and standalone methods. Notwithstanding the elevated computational expenses, the hybrid approach proves especially beneficial in volatile circumstances where improved accuracy and interpretability warrant the additional cost.

The effectiveness of MOGWO, MOPSO, and MOLA was assessed in terms of accuracy, convergence speed, computational efficiency, and scalability. Table 3 demonstrates that MOGWO surpassed the other methods in terms of accuracy (exhibiting the lowest RMSE and MAE) and computational efficiency (achieving the quickest convergence). MOGWO has shown exceptional durability and scalability, rendering it the ideal selection for multi-objective optimization in natural gas dehydration. Although MOPSO exhibited a somewhat elevated R^2 value, MOGWO demonstrated a more equitable performance across all parameters, demonstrating its supremacy.

Table 3: Comparison of metaheuristic algorithms based on evaluation criteria.

Evaluation Criteria	**MOGWO**	**MOPSO**	**MOLA**	**Best Algorithm**
Accuracy (RMSE)	0.0194	0.0223	0.0263	MOGWO
Accuracy (MAE)	0.0139	0.0186	0.0230	MOGWO
Accuracy (R^2)	0.9937	0.9942	0.9879	MOPSO
Convergence Speed	Fast (Low computational time)	Moderate	Moderate	MOGWO
Computational Efficiency	High (Lower time complexity)	Moderate	Moderate	MOGWO
Scalability	High (Handles large datasets well)	Moderate	Moderate	MOGWO
Robustness (Diversity)	High (Best diversity of solutions)	Moderate	Moderate	MOGWO
Generalization (Out-of-Sample Accuracy)	92%	87%	89%	MOGWO

The computational efficiency of the hybrid model is essential for real-time decision-making in natural gas processing. The convergence time and computational resources necessary for optimization were evaluated. MOGWO surpassed MOPSO and MOLA in convergence velocity, necessitating reduced time on a typical server. Scalability studies demonstrated that MOGWO preserved efficiency as problem complexity escalated, with its computing time increasing linearly, whereas the other algorithms displayed more substantial increases. MOGWO is ideally suited for extensive, real-time applications in natural gas processing, providing results within the requisite timeframes for industrial utilization. Table 4 delineates the computing efficacy of the three algorithms, illustrating MOGWO's preeminence in convergence time, CPU utilization, memory usage, and real-time processing velocity, so establishing it as the ideal selection for real-time decision-making in natural gas dehydration.

Table 4: Computational performance of algorithms.

Algorithm	**Convergence Time (min)**	**CPU Usage (%)**	**Memory Usage (MB)**	**Real-Time Processing Time**
MOGWO	10	60	350	2
MOPSO	12	65	380	3
MOLA	14	70	400	3.5

4 Conclusion

With the increase in the production, transmission, distribution, and consumption of NG, the importance of producing gas free from impurities increases. The gas extracted from the fields has some impurities. The NG obtained from the tank includes compounds such as methane, NG liquids, CO_2, H_2S, and water. Water is one of these abnormalities, and its presence in the gas causes many problems in the next stages, including transmission. The existence of strict environmental laws regarding the emission of compounds such as benzene, toluene, ethyl benzene, and xylene (BTEX) shows the importance of the emission of these compounds in the oil and gas industries. Therefore, in refineries, NG processing takes place in two main units, including acid gas eradication (including CO_2 and H_2S) and water removal (dehydration unit). In this study, two main goals are considered, i.e., trying to diminish BTEX emissions (environmental protection) and maintaining the traits of dry gas water contents (economic sustainability). Therefore, in this study, by presenting a multi-objective enhancement approach was presented to identify the optimal values to minimize the BTEX releases and maintain the traits of dry gas water contents. For this purpose, three frameworks, MOGWO, MOLA, and MOPSO, were used to solve the multi-objective optimization problem. To improve the accuracy of predictions, four optimization frameworks, including GRU, MLP, RF, and SVR, were used to optimize and hyper-adjust the parameters of the main frameworks. Therefore, by combining different frameworks, 12 different hybrid models were investigated to solve the optimization problem raised in this study. The LINMAP method was used to calculate the distance between the ideal point and the LINMAP point to choose the best algorithm to solve the multi-objective optimization problem. After choosing the best multi-objective optimization problem, the evaluation indices were calculated and compared to assess the best optimization algorithm. The outcomes of the case study showed that among the three main frameworks recommended to solve the optimization problem, the MOGWO algorithm had the best performance based on the LINMAP method. Also, the examination and comparison of different evaluation indices showed that the RF algorithm had the best values of the evaluation indices except for R^2 in predicting the BTEX variable. Also, considering the Dry Gas Water Content variable, RF and SVR frameworks have been better than others. Therefore, in this study, the MOGWO-RF hybrid model is recommended to solve the multi-objective optimization problem related to NG processing.

Funding

This research received no specific grant from any funding agency in the public, commercial, or not-for-profit sectors.

Appendix

The execution of the MOGWO, MOPSO, and MOLA algorithms, their integration with machine learning models (GRU, MLP, RF, SVR), and the optimization procedure are detailed, covering initialization, data preprocessing, evaluation metrics, and computational efficiency. It includes server specifications and scalability assessments to ensure real-time applicability in natural gas processing. This structure provides a clear framework for replicating the model's implementation and evaluation.

Nomenclature

ANN	Artificial Neural Network	NG	Natural Gas
$\vec{A}$	Coefficient vectors	num	Number of observations
$\vec{a}$	Coefficient of convergence	PSO	Particle Swarm Optimization
b	Bias vector	P_{bi}	Best previous fitness values
COS	Carbonyl sulfide	r_1, r_2,..	Random number
CO_2	Carbon dioxide	r	Updated gate in GRU
$\vec{C}$	Coefficient vectors	r_t	A reset gate
c_1	Cognition learning factor	SVR	Support Vector Regression
c_2	Coefficient of social acceleration	TEG	Tri Ethylene Glycol
DL	Deep Learning	u_i	The upper bound of xi
DEG	Di Ethylene Glycol	V_i^k	Location of i_{th} particle in iteration k
$\vec{D}$	Distance from the wolf to the prey	VOC	Volatile Organic Compounds
f_{BTEX}	Variables related to BTEX	v_i	i_{th} detected value
f_{dryW}	Variables related to dry gas water content	$\hat{v}_i$	i_{th} expected value
GRU	Gated Recurrent Unit	$\bar{v}$	Average of observations
GWO	Gray Wolf Algorithm	ω	Weight vector
G_{bi}	The best position of particle i	w_{fBTEX}	Parameter of f_{BTEX}
g	Inequality limits	w_{fdryW}	Parameter of $f_{dryW.}$
H_2S	Hydrogen sulfur	w'	Inertia weight factor
$\tilde{h}_t$	Selected activation function at time t	$w_{i,j}$	Weight
h	Equality limits	$\overrightarrow{X_p}$	Position vector of the prey

h_t	Activation function at time t	$\vec{X}(t)$	Hunting position at the moment t
L	Number of neurons	X_i^k	The velocity of i_{th} particle in iteration k
l_i	The lower bound of x_i	x	Vector of the variables
MLP	Multi-Layer Perceptron	y_{BTEX}	BTEX emission
M	Responsible parameter for balancing the simplicity of the framework with error value	y_{dryW}	Dry gas water content
MOP	Multi-objective Optimization Problem	z	Reset gate in GRU
MCDM	multi-criteria decision-making	z_t	Update Gate Vector
MOGWO	Multi-Objective Grey Wolf Optimizer	φ	Numerical constant
MOLA	Multi-Objective land allocation	ξ_i^* and ξ_i	Auxiliary variables
MOPSO	Multi-Objective Particle Swarm Optimization	ε'	Width of the tube.

References

[1] S. Kanwal, M. T. Mehran, M. Hassan, M. Anwar, S. R. Naqvi, and A. H. Khoja, "An integrated future approach for the energy security of Pakistan: Replacement of fossil fuels with syngas for better environment and socio-economic development," *Renewable and Sustainable Energy Reviews*, vol. 156, p. 111978, 2022.

[2] C. Antonini, K. Treyer, A. Streb, M. van der Spek, C. Bauer, and M. Mazzotti, "Hydrogen production from natural gas and biomethane with carbon capture and storage–A techno-environmental analysis," *Sustain Energy Fuels*, vol. 4, no. 6, pp. 2967–2986, 2020.

[3] C. Gürsan and V. de Gooyert, "The systemic impact of a transition fuel: Does natural gas help or hinder the energy transition?" *Renewable and Sustainable Energy Reviews*, vol. 138, p. 110552, 2021.

[4] C. Tan, M. Wang, R. Chen, and F. You, "Study on the Oil Well Cement-Based Composites to Prevent Corrosion by Carbon Dioxide and Hydrogen Sulfide at High Temperature," *Coatings*, vol. 13, no. 4, p. 729, 2023.

[5] M. Rahmani, B. Mokhtarani, M. Mafi, and N. Rahmanian, "Acid gas removal by superhigh silica ZSM-5: Adsorption isotherms of hydrogen sulfide, carbon dioxide, methane, and nitrogen," *Ind Eng Chem Res*, vol. 61, no. 19, pp. 6600–6610, 2022.

[6] S. M. Alardhi, T. Al-Jadir, A. M. Hasan, A. A. Jaber, and L. M. Al Saedi, "Design of Artificial Neural Network for Prediction of Hydrogen Sulfide and Carbon Dioxide Concentrations in a Natural Gas Sweetening Plant.," *Ecological Engineering & Environmental Technology (EEET)*, vol. 24, no. 2, 2023.

[7] J. R. Heller, "Reliability Analysis of Acid Gas Removal Units A comparative study of conventional and emerging natural gas purification technologies," 2022, *uis*.

[8] T. Ariadji, S. Adisasmito, L. Mucharam, and D. Abdassah, "Improved Joule Thomson equation of supercritical CO2-rich natural gas in separation system," *Natural Gas Industry B*, 2023.

[9] A. Pudi, M. Rezaei, V. Signorini, M. P. Andersson, M. G. Baschetti, and S. S. Mansouri, "Hydrogen sulfide capture and removal technologies: A comprehensive review of recent developments and emerging trends," *Sep Purif Technol*, vol. 298, p. 121448, 2022.

[10] F. Santoni *et al.*, "Hydrogen Sulphide and Carbonyl Sulphide Removal from Biogas for Exploitation in High-Temperature Fuel Cells," *Waste Biomass Valorization*, pp. 1–21, 2023.

[11] L. Hou, W. Ma, X. Luo, J. Liu, S. Liu, and Z. Zhao, "Hydrocarbon generation-retention-expulsion mechanism and shale oil producibility of the permian lucaogou shale in the Junggar Basin as simulated by semi-open pyrolysis experiments," *Mar Pet Geol*, vol. 125, p. 104880, 2021.

[12] S. Duval, "Natural gas sweetening," in *Surface Process, Transportation, and Storage*, Elsevier, 2023, pp. 37–78.

[13] Y. Liu *et al.*, "Effect and mechanisms of red mud catalyst on pyrolysis remediation of heavy hydrocarbons in weathered petroleum-contaminated soil," *J Environ Chem Eng*, vol. 9, no. 5, p. 106090, 2021.

[14] E. Nikooei, N. AuYeung, I. Lima, X. Tan, A. Benard, and B. Abbasi, "Separation of volatile organic contaminants from water using a direct-contact dehumidifier: An experimental study and modeling," *Journal of Water Process Engineering*, vol. 52, p. 103520, 2023.

[15] W. Zhang, P. Xie, Y. Li, L. Teng, and J. Zhu, "Hydrodynamic characteristics and mass transfer performance of rotating packed bed for CO2 removal by chemical absorption: A review," *J Nat Gas Sci Eng*, vol. 79, p. 103373, 2020.

[16] H. Shadanfar, A. Elhambakhsh, and P. Keshavarz, "Air dehumidification using various TEG based nano solvents in hollow fiber membrane contactors," *Heat and Mass Transfer*, vol. 57, pp. 1623–1631, 2021.

[17] S. Notter, C. Donsbach, and C. Feldmann, "On iodido bismuthates, bismuth complexes and polyiodides with bismuth in the system BiI3/18-

crown-6/I2," *Zeitschrift für Naturforschung B*, vol. 76, no. 10–12, pp. 765–774, 2021.

[18] E. Kusrini, W. W. Prihandini, F. A. Jatmoko, A. Usman, and Y. Muharam, "Feasibility study of CO2 purification using pressure swing adsorption and triethylene glycol absorption for enhanced oil recovery," in *AIP Conference Proceedings*, AIP Publishing, 2020.

[19] N. A. Darwish, R. A. Al-Mehaideb, A. M. Braek, and R. Hughes, "Computer simulation of BTEX emission in natural gas dehydration using PR and RKS equations of state with different predictive mixing rules," *Environmental Modelling & Software*, vol. 19, no. 10, pp. 957–965, 2004.

[20] N. A. Darwish and N. Hilal, "Sensitivity analysis and faults diagnosis using artificial neural networks in natural gas TEG-dehydration plants," *Chemical Engineering Journal*, vol. 137, no. 2, pp. 189–197, 2008.

[21] U. Eldemerdash and K. Kamarudin, "Assessment of new and improved solvent for pre-elimination of BTEX emissions in glycol dehydration processes," *Chemical Engineering Research and Design*, vol. 115, pp. 214–220, 2016.

[22] M. A. Torkmahalleh, G. Magazova, A. Magazova, and S. J. H. Rad, "Simulation of environmental impact of an existing natural gas dehydration plant using a combination of thermodynamic models," *Process Safety and Environmental Protection*, vol. 104, pp. 38–47, 2016.

[23] E. G. Petropoulou, C. Carollo, G. D. Pappa, G. Caputo, and E. C. Voutsas, "Sensitivity analysis and process optimization of a natural gas dehydration unit using triethylene glycol," *J Nat Gas Sci Eng*, vol. 71, p. 102982, 2019.

[24] N. Tazang, F. Alavi, and J. Javanmardi, "Estimation of solubility of BTEX, light hydrocarbons and sour gases in triethylene glycol using the SAFT equation of state," *Physical Chemistry Research*, vol. 8, no. 2, pp. 251–266, 2020.

[25] R. Mukherjee and U. M. Diwekar, "Multi-objective optimization of the TEG dehydration process for BTEX emission mitigation using machine-learning and metaheuristic algorithms," *ACS Sustain Chem Eng*, vol. 9, no. 3, pp. 1213–1228, 2021.

[26] R. Mukherjee and U. M. Diwekar, "Optimizing TEG dehydration process under metamodel uncertainty," *Energies (Basel)*, vol. 14, no. 19, p. 6177, 2021.

[27] R. Mukherjee, "Reliability-based robust multi-objective optimization (RBRMOO) of chemical process systems: a case study of TEG dehydration plant," *Frontiers in Sustainability*, vol. 3, p. 856836, 2022.

[28] R. Mukherjee and U. M. Diwekar, "Multi-objective optimization of the TEG dehydration process for BTEX emission mitigation using machine-learning and metaheuristic algorithms," *ACS Sustain Chem Eng*, vol. 9, no. 3, pp. 1213–1228, 2021.

[29] F. Wang, J. Zhao, and V. Van Hoang, "Prediction of variables involved in TEG Dehydration using hybrid models based on boosting algorithms," *Comput Chem Eng*, vol. 188, p. 108747, 2024, doi: https://doi.org/10.1016/j.compchemeng.2024.108747.

[30] C. Liu *et al.*, "A modified multi-objective grey wolf optimizer for multi-objective flood control operation of cascade reservoirs," *J Hydrol (Amst)*, vol. 658, p. 133162, 2025, doi: https://doi.org/10.1016/j.jhydrol.2025.133162.

[31] W. Sun, Y. Wang, L. Zhang, X. H. Chen, and Y. H. Hoang, "Enhancing economic cycle forecasting based on interpretable machine learning and news narrative sentiment," *Technol Forecast Soc Change*, vol. 215, p. 124094, 2025, doi: https://doi.org/10.1016/j.techfore.2025.124094.

[32] Y. Luo, Y. Liu, J. Chen, J. Yang, and J. Yu, "Multi-objective particle swarm algorithm based on angular segmentation archive and dynamic update tactics," *Sci Rep*, vol. 15, no. 1, p. 31012, 2025, doi: 10.1038/s41598-025-16539-8.

[33] C. J. Davidson, J. H. Hannigan, and S. E. Bowen, "Effects of inhaled combined Benzene, Toluene, Ethylbenzene, and Xylenes (BTEX): Toward an environmental exposure model," *Environ Toxicol Pharmacol*, vol. 81, p. 103518, 2021.

[34] R. Mukherjee and U. M. Diwekar, "Multi-objective optimization of the TEG dehydration process for BTEX emission mitigation using machine-learning and metaheuristic algorithms," *ACS Sustain Chem Eng*, vol. 9, no. 3, pp. 1213–1228, 2021.

[35] J. J. Thakkar, *Multi-criteria decision making*, vol. 336. Springer, 2021.

[36] M. A. Haghghi, A. Hasanzadeh, E. Nadimi, A. Rosato, and H. Athari, "An intelligent thermodynamic/economic approach based on artificial neural network combined with MOGWO algorithm to study a novel polygeneration scheme using a modified dual-flash geothermal cycle," *Process Safety and Environmental Protection*, vol. 173, pp. 859–880, 2023, doi: https://doi.org/10.1016/j.psep.2023.03.056.

[37] S. Mirjalili, S. M. Mirjalili, and A. Lewis, "Grey wolf optimizer," *Advances in engineering software*, vol. 69, pp. 46–61, 2014.

[38] Y. Meraihi, A. B. Gabis, S. Mirjalili, and A. Ramdane-Cherif, "Grasshopper optimization algorithm: theory, variants, and applications," *IEEE Access*, vol. 9, pp. 50001–50024, 2021.

[39] M. Song and D. Chen, "An improved knowledge-informed NSGA-II for multi-objective land allocation (MOLA)," *Geo-spatial Information Science*, vol. 21, no. 4, pp. 273–287, 2018.

[40] G. Liu, Y. Zhu, S. Xu, Y.-C. Chen, and H. Tang, "PSO-based power-driven X-routing algorithm in

semiconductor design for predictive intelligence of IoT applications," *Appl Soft Comput*, vol. 114, p. 108114, 2022.

[41] A. G. Gad, "Particle swarm optimization algorithm and its applications: a systematic review," *Archives of computational methods in engineering*, vol. 29, no. 5, pp. 2531–2561, 2022.

[42] A. Djouahi, B. Negrou, B. Rouabah, A. Mahboub, and M. M. Samy, "Optimal Sizing of Battery and Super-Capacitor Based on the MOPSO Technique via a New FC-HEV Application," *Energies (Basel)*, vol. 16, no. 9, p. 3902, 2023.

[43] R. Eberhart and J. Kennedy, "Particle swarm optimization," in *Proceedings of the IEEE international conference on neural networks*, Citeseer, 1995, pp. 1942–1948.

[44] K. Cho, B. Van Merriënboer, D. Bahdanau, and Y. Bengio, "On the properties of neural machine translation: Encoder-decoder approaches," *arXiv preprint arXiv:1409.1259*, 2014.

[45] J. Chung, C. Gulcehre, K. Cho, and Y. Bengio, "Empirical evaluation of gated recurrent neural networks on sequence modeling," *arXiv preprint arXiv:1412.3555*, 2014.

[46] S. Wang, J. Chen, H. Wang, and D. Zhang, "Degradation evaluation of slewing bearing using HMM and improved GRU," *Measurement*, vol. 146, pp. 385–395, 2019.

[47] A. H. Alavi and A. H. Gandomi, "Prediction of principal ground-motion parameters using a hybrid method coupling artificial neural networks and simulated annealing," *Comput Struct*, vol. 89, no. 23–24, pp. 2176–2194, 2011.

[48] A. Rezaeipanah and G. Ahmadi, "Breast cancer diagnosis using multi-stage weight adjustment in the MLP neural network," *Comput J*, vol. 65, no. 4, pp. 788–804, 2022.

[49] C. M. Bishop, *Neural networks for pattern recognition*. Oxford university press, 1995.

[50] A. Sarica, A. Cerasa, and A. Quattrone, "Random forest algorithm for the classification of neuroimaging data in Alzheimer's disease: a systematic review," *Front Aging Neurosci*, vol. 9, p. 329, 2017.

[51] A. Liaw and M. Wiener, "Classification and regression by randomForest," *R news*, vol. 2, no. 3, pp. 18–22, 2002.

[52] N. Dogru and A. Subasi, "Traffic accident detection using random forest classifier," in *2018 15th learning and technology conference (L&T)*, IEEE, 2018, pp. 40–45.

[53] H. Drucker, C. J. Burges, L. Kaufman, A. Smola, and V. Vapnik, "Support vector regression machines," *Adv Neural Inf Process Syst*, vol. 9, 1996.

[54] H. Yu and S. Kim, "SVM Tutorial-Classification, Regression and Ranking.," *Handbook of Natural computing*, vol. 1, pp. 479–506, 2012.

[55] E. Ghasemi, H. Kalhori, and R. Bagherpour, "A new hybrid ANFIS–PSO model for prediction of peak particle velocity due to bench blasting," *Eng Comput*, vol. 32, pp. 607–614, 2016.

[56] H. Khajavi and A. Rastgoo, "Predicting the carbon dioxide emission caused by road transport using a Random Forest (RF) model combined by Meta-Heuristic Algorithms," *Sustain Cities Soc*, vol. 93, p. 104503, 2023, doi: https://doi.org/10.1016/j.scs.2023.104503.